energies

MDPI

Article

Knockout of the Aldehyde Dehydrogenase Gene in *Fusarium oxysporum* for Enhanced Ethanol Yield

Jinxia Fan [1,2], Xiaomei Huang [3], Guoxiang Zheng [1,2], Changyu Liu [1,2], Ming Wang [1,2], Yong Sun [1,2] and Qian Yang [4,*]

[1] College of Engineering, Northeast Agricultural University, Harbin 150030, China
[2] Key Laboratory of Swine Facilities Engineering, Ministry of Agriculture and Rural Affairs, Harbin 150030, China
[3] Department of Bioengineering, Heilongjiang Vocational College of Agricultural Technology, Jiamusi 154007, China
[4] Department of Life Science and Engineering, Harbin Institute of Technology, Harbin 150001, China
* Correspondence: yangq20112022@126.com; Tel.: +86-155-4598-5760

Abstract: Acetic acid is the primary by-product generated from ethanol production by *Fusarium oxysporum* using glucose or xylose as a substrate. Aldehyde dehydrogenase (ALDH) is the critical enzyme in acetic acid metabolism. To decrease acetic acid yield in ethanol production, the 1509 bp DNA of *aldh*, encoding a 502 amino acid protein with a calculated molecular mass of 54.33 kDa and an isoelectric point of 6.21, was cloned from *F. oxysporum*. Sequence analysis confirmed that the screened proteins belonged to the ALDH family. A knockout vector, Δ*aldh*, containing positive (hygromycin resistance gene) and negative (thymidine kinase gene from the herpes simplex virus) selectable markers, was constructed. Ethanol production by the mutant (cs28pCAM-Pstal-Δ*aldh*) in glucose- and xylose-containing media was 0.46 and 0.39 g/g, respectively, and these yields were 16.93% and 34.63% higher than those by the wild-type strain (0.393 and 0.289 g/g). Furthermore, the acetic acid yield of the mutant was 3.50 and 3.01 g/L, respectively, showing a 23.10% and 39.55% decrease compared with the wild-type strain (4.308 and 4.196 g/L). The biomass of the mutant (4.05 and 4.52 g/L) was lower than that of the wild-type strain (4.71 and 5.97 g/L). These results demonstrated the potential use of the genetically stable mutant for industrial bioethanol production.

Keywords: aldehyde dehydrogenase; *Fusarium oxysporum*; gene knockout; acetic acid

Citation: Fan, J.; Huang, X.; Zheng, G.; Liu, C.; Wang, M.; Sun, Y.; Yang, Q. Knockout of the Aldehyde Dehydrogenase Gene in *Fusarium oxysporum* for Enhanced Ethanol Yield. *Energies* **2023**, *16*, 427. https://doi.org/10.3390/en16010427

Academic Editor: Fernando Rubiera González

Received: 17 November 2022
Revised: 6 December 2022
Accepted: 27 December 2022
Published: 30 December 2022

1. Introduction

Lignocellulose is a major component of biomass, comprising approximately half of the plant matter produced by photosynthesis and representing the most abundant renewable organic resource in soil. Annual lignocellulosic residue generation worldwide results in environmental pollution and loss of valuable materials that can be bioconverted to several value-added products [1], such as bioethanol. Lignocellulose primarily consists of three types of polymers, namely cellulose, hemicellulose, and lignin, which can be hydrolyzed and depolymerized using enzyme-mimicking nanoparticles for enhanced bioethanol production [2,3]. The prerequisite for using this method is to use an enzyme with high enzymatic activity.

Fusarium oxysporum is a species that is pathogenic in plants and not in humans/animals, possessing bio-control activity against fungal pests, some insects, and metabolites [4,5]. This species can infiltrate the lignin barrier of plants and express various enzymes, including cellulose, xylanase, β-glucosidase, pectinase, laccase, and lignin peroxidase, making it a promising microbial agent in consolidated bioprocessing systems [6,7]. It can convert glucose and xylose into ethanol [8] (Figure 1) and simultaneously saccharify cellulose to ethanol [9]. However, the ethanol production efficiency of *F. oxysporum* is low. To improve its ability to convert substrates to ethanol, several genetic mutants of *F. oxysporum* were

constructed by overexpressing different enzymes of the sugar transporter [6,10], pentose phosphate [11,12], or Embden–Meyerhof–Parnas [13] pathways. However, acetate, a by-product of glucose and xylose fermentation by *F. oxysporum*, also leads to low ethanol yield.

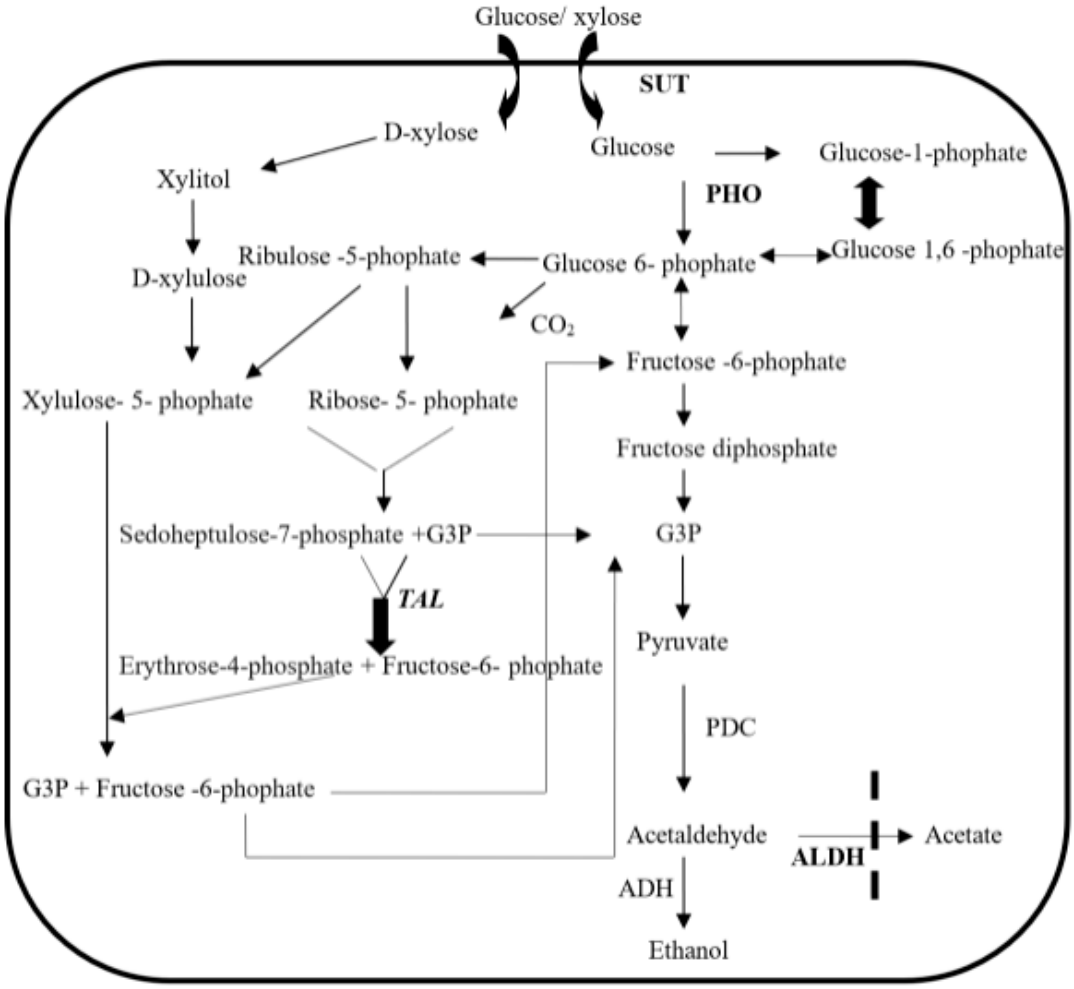

Figure 1. Metabolic pathways for glucose and xylose in *F. oxysporum* [10,12,13].

Aldehyde dehydrogenase (ALDH) (EC 1.2.1.5) converts acetaldehyde into acetate. It is generally accepted that ALDH can only catalyze acetaldehyde oxidation, i.e., it is unable to reduce acetate; thus, this reaction is irreversible. This enzyme participates in ethanol metabolism in numerous microorganisms, such as *Thermoanaerobacter ethanolicus* and *Natronomonas pharaonis* [14,15]. Control of *aldA* expression is crucial for the initiation and maintenance of an optimal catabolic flow from ethanol in *Aspergillus nidulans* [16]. In *Saccharomyces cerevisiae,* Ald4p and Ald6p function in the production of acetate from acetaldehyde and are thus critical in acetyl-CoA production [17]. ALDH1 and ALDH2 catalyze the oxidation of the acetaldehyde produced during fermentation in *S. cerevisiae* [18]. In an *aldh* knockout mutant of *S. cerevisiae*, the acetic acid yield decreased [19]. In this study, we attempted to change the metabolic path of acetic acid to increase the ethanol yield of *F. oxysporum*.

The aim of this study was to investigate the ethanol yield in an *F. oxysporum* mutant strain during glucose or xylose fermentation, and to examine the possibility of increasing it via the deletion *aldh*. The engineered mutant strain may be a candidate microorganism with high ethanol yield for use in bioconversion processes.

SUT, sugar transporter; PHO, phosphoglucomutase; TAL, transaldolase; G3P, glyceraldehydes-3-phosphate; PDC, pyruvate dehydrogenase; ADH, alcohol dehydrogenase; ALDH, aldehyde dehydrogenase.

2. Materials and Methods

2.1. Strains, Plasmids, and Growth Conditions

Fusarium oxysporum cs28 strain was stored in our laboratory. *Fusarium oxysporum* cs28pCAM-Pstal strain harboring the transaldolase (*tal*) from *Pichia stipitis* was used as a recipient strain for transformation [11]. *Agrobacterium tumefaciens* EHA105 (Mingzhoubio Co., Ltd., China) was used for *Agrobacterium*-mediated transformation and grown in Luria-Bertani medium containing kanamycin (50 μg/mL) at 28 °C. *Escherichia coli* DH5α (Invitrogen, USA) was used for the construction, propagation, and amplification of plasmids and grown at 37 °C in Luria-Bertani medium containing either ampicillin (100 μg/mL) or kanamycin (50 μg/mL), depending on the resistance marker of the plasmid used. The plasmids pUC18 (Takara, Japan), pCSN43 [20], and pPZPtk8.10 [21] were used to construct the homogenous recombinant vector.

2.2. Cloning and Bioinformation Analysis of the aldh Gene

Using the ALDH protein sequence of *Neurospora crassa* [13], the sequenced *F. oxysporum* genome (http://www.broad.mit.edu/annotation/genome/fusarium_group/MultiHome.html (accessed on 8 May 2019)) was scanned using the Basic Local Alignment Search Tool (BLAST). This revealed a 502-residue aldh protein with 82% amino acid sequence identity. Based on the *aldh* sequence of *F. oxysporum*, primers AldF (5′-CGA ATC ATC ATA CAT CCA CAA TG-3′) and AldR (5′-GAG TAT TTT GGT ACA GAT AGA CC-3′) were designed and used to isolate the relevant gene from *F. oxysporum* genomic DNA. The PCR product was amplified using a high-fidelity polymerase (Takara, Japan). The 1.6 kb PCR product was cloned into the cloning vector pMD18-T and then sequenced.

The open reading frame of the *aldh* was searched using the ORF program (http://www.ncbi.nlm.nih.gov/gorf/gorf.html (accessed on 11 August 2019)). The theoretical molecular mass and isoelectric point of the ALDH were calculated using the Protparam tool (http://us.expasy.org/tools/protparam.html (accessed on 11 August 2019)). The catalytic domain of the ALDH was identified by InterProScan (http://www.ebi.ac.uk/Tools/InterProScan/ (accessed on 11 August 2019)). ALDH amino acid sequences from different fungi were aligned using the MultAlin program (http://multalin.toulouse.inra.fr/multalin (accessed on 3 December 2022)).

2.3. Construction of Homogenous Recombinant Plasmid and Transformation

Firstly, *aldh* was obtained using PCR amplification with P1 and P2 primers and the genomic DNA of *F. oxysporum* as a template. The gene was digested using the restriction enzymes *Eco*RI and *Bam*HI (Roche, Mannheim, Germany). The fragment was inserted into *Eco*RI and *Bam*HI-cut pUC18, resulting in the plasmid pUC-*aldh*. Secondly, the hygromycin B resistance (*hyB*) gene cassette was obtained by PCR amplification using pCSN43 as a template and primers P3 and P4. The *hyB* gene cassette was then digested using *Nhe*I (Roche, Germany) and inserted into plasmid pUC-*aldh*, yielding the plasmid pUC-*aldh-hyB*. Thirdly, the *aldh* gene containing *hyB* gene cassette was amplified with primers P5 and P6 using the pUC-*aldh-hyB* plasmid as a template. The PCR fragment was subsequently digested using the restriction enzyme *Kpn*I (Roche, Germany) and inserted into pPZPtk8.10, resulting in the binary homogenous recombinant vector pPZP-*aldh-hyB*. Table 1 outlines the primers of the construction vector used for targeted mutations of *aldh*.

The vectors pPZP-*aldh-hyB* and pPZPtk8.10 were transformed into *A. tumefacients* EHA105 using the freeze-thaw method [22], and transformants were selected on LB medium containing 100 μg/mL kanamycin, 50 μg/mL streptomycin, and 20 μg/mL rifampicin. The pPZP-*ald-hyB* vector was extracted from the transformants of *A. tumefacients*, identified using PCR with P5 and P6 primers, and then digested using the restriction enzyme *KpnI* (Roche, Germany).

Table 1. Primers used in this study.

Primer Designation	Sequence (5′-3′)	Restricted Enzyme
P1	5′CCGGAATTCCGAATCATCATACATCCACAATG3′	*Eco*RI
P2	5′CGGGATCCGAGTATTTTGGTACAGATAGACC3′	*Bam*HI
P3	5′CTAGCTAGCCCCTCGAGGTCGACAGAAGATGATA3′	*Nhe*I
P4	5′CTAGCTAGCTCCGGCGTAGAGGATCCTCTAGAAA3′	*Nhe*I
P5	5′GGGGTACCCGAATCATCATACATCCACAATGAGTCTAG3′	*Kpn*I
P6	5′GGGGTACCGAGTATTTTGGTACAGATAGACCATCTTCTC3′	*Kpn*I
P7	5′-CGGAAGCGAGAAACATCTCCTTAT-3′	
P8	5′-AAGCTGAAAGCACGAGATTCTTCG-3′	

Restriction sites are shown in lowercase.

2.4. Agrobacterium Tumefaciens-Mediated Transformation and Screening of Fungal Mutants

Plasmid pPZP-*aldh-hyB* or pPZPtk8.10 (control) was transformed into *F. oxysporum* strain cs28pCAM-Ptal using *Agrobacterium tumefaciens* EHA105 strain as a mediator, as described previously by Covert et al. [23].

Fungal genomic DNA was isolated as described by Karakousis [24]. The putative knockout mutants were screened in two steps. In the first step, the transformed *F. oxysporum* was cultured on dual selection plates, namely potato dextrose agar plates containing 100 μg/mL hygromycin (Roche, Germany) and 10 μM F2dU (Roche, Germany). In the second step, putative knockout mutants were screened from the dual selection plates using PCR with specific primer pairs P7/P8 and P1/P2 (Table 1). The PCR cycling conditions were 94 °C for 5 min; 94 °C for 30 s, 53 °C for 30 s, and 72 °C for 1 min for 32 cycles; and 72 °C for 10 min. The PCR product was then cloned into the pMD18-T vector and sequenced by Sangon Biotech Co., Ltd., Shanghai, China. The mutant strain was designated as cs28pCAM-Ptal-Δ*aldh*.

2.5. Genetic Stability of Transformants

To test the mitotic stability of the disrupted *aldh* in the *F. oxysporum* transformants, spores of the transformants were inoculated into 3 mL of PX medium (xylose, 20 g/L; potato, 200 g/L) and incubated at 28 °C with shaking at 120 rpm. After 4 days of growth, 50 μL of each culture was plated on potato xylose agar containing 50 μL/mL hygromycin B or on unamended potato xylose agar. Additionally, mitotic stability was tested on solid cultures by transferring the mycelium of each transformant to one edge of a PXA (xylose, 20 g/L; potato, 200 g/L; agar, 20 g/L) plate. Once the growth reached the opposite side of the plate, mycelium from the growing edge was transferred to PXA containing 50 μL/mL hygromycin B or to unamended PXA.

2.6. Fermentation Conditions

Fusarium oxysporum strain cs28 and mutant cs28pCAM-Ptal-Δ*aldh* were prepared using PX medium (xylose, 20 g/L; potato, 200 g/L) at 30 °C with shaking at 140 rpm for 24 h. Glucose (20 g/L) and xylose (20 g/L) media were prepared separately. The composition of the fermentation media (pH 6.0) excluding the sugars was (g/L): yeast extract, 2; $NaNO_3$, 10; $MgSO_4$, 0.2; KH_2PO_4, 2; and $CaCl_2$, 0.1. Fermentation was performed in sterile 100 mL Erlenmeyer flasks at 30 °C. Each Erlenmeyer flask contained 50 mL of sugar medium and 5 mL of inoculum. All media were autoclaved at 121 °C for 20 min before use. Samples of the culture were taken at different time intervals.

2.7. Analytical Methods

The dried cell mass was measured from 50 mL of cell suspension. The suspension was centrifuged, and the cell pellet was washed twice with distilled water and oven-dried overnight at 105 °C. The first supernatant was analyzed for ethanol and acetic acid concentrations using gas chromatography. Ethanol and acetic acid concentrations were

measured using a GC-4890 gas chromatograph (Agilent, Palo Alto, CA, USA) equipped with an Inwax capillary column (Agilent, USA) and a flame ionization detector. Gas chromatography was conducted at an oven temperature of 70 °C and injection temperature of 200 °C with nitrogen as a carrier gas and hydrogen as a flaming gas. Glucose and xylose concentrations were determined using the 3,5-dinitrosalicylic acid method [25]. Analysis of variance was performed using SAS 9.0 (SAS Inc., Kerry, NC, USA).

3. Results and Discussion

3.1. Cloning and Sequence Analysis of aldh

The coding region of *aldh* was 1509 bp in length. It encoded 502 amino acids and had a calculated molecular mass of 54.33 kDa and a predicted isoelectric point of 6.21. The *aldh* sequence was deposited in the GenBank database with the accession number ACN65117. InterProScan analysis revealed that aldh had conserved ALDH active sites (InterPro acc. no. IPR016160), indicating that it is an ALDH.

Multiple sequence alignment of ALDH from 20 fungal species was conducted using the MultAlin program, and the results revealed that the amino acid sequences of these ALDHs were conserved, with identities ranging from 47% to 98%. Furthermore, the active sites of these different ALDHs were highly conserved. The consensus sequence of conserved site and NAD(P) binding site was TLE [T/L] GGKSP and IIPWN/W/K/AE/FTGS, respectively (Figure 2).

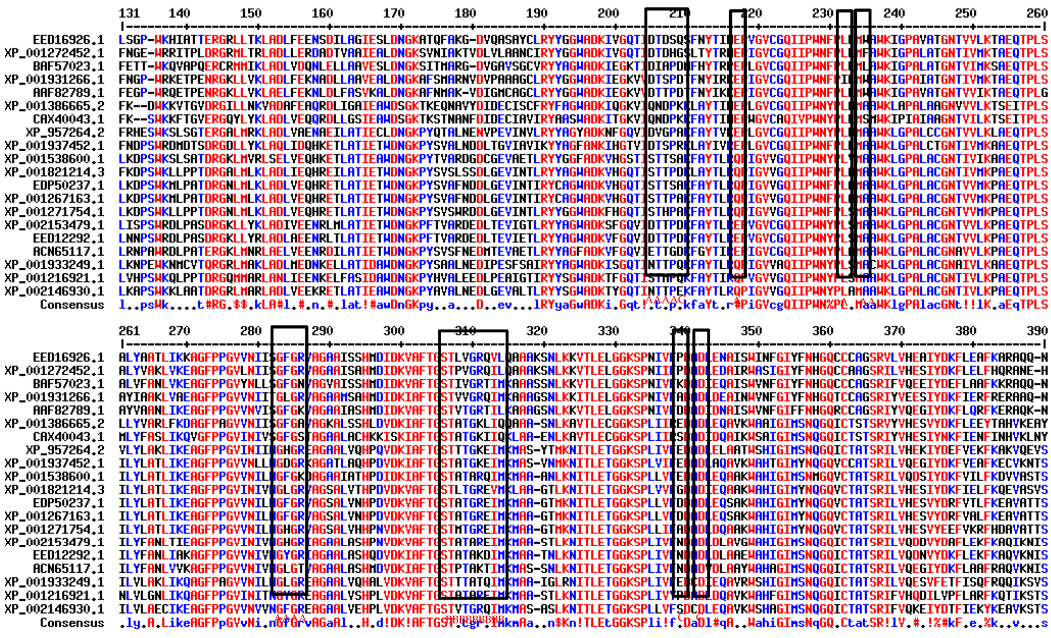

Figure 2. Multiple sequence alignment of conserved domain of aldehyde dehydrogenase from 20 fungal species. All of these aldehyde dehydrogenases are members of the aldehyde dehydrogenase superfamily; their active sites and chemical binding sites are highly conserved. The asterisks refer to the conserved amino acid residues. A: NAD(P) binding site; B: active site; C: active site and NAD(P) binding site.

XP_002146930: Penicillium marneffei; XP_001216921: Aspergillus terreus; XP_001933249: Pyrenophora triticirepentis; ACN65117: Fusarium oxysporum; EED12292: Talaromyces stipitatus; XP_002153479: Penicillium marneffei; XP_001267163: Neosartorya fischeri; EDP50237: Aspergillus fumigatus; XP_001271754: Aspergillus clavatus; XP_001821214: Aspergillus oryzae; XP_001538600: Ajellomyces capsulatus; XP_001937452: Pyrenophora triticirepentis; XP_957264: Neurospora crassa; CAX40043: Candida dubliniensis; XP_001386665: Pichia stipitis; AAF82789: Cladosporium fulvum; XP_001931266: Pyrenophora triticirepentis; BAF57023: Aciculosporium take; XP_001272452: Aspergillus clavatus; EED16926: Talaromyces stipitatus.

3.2. Disruption of aldh in F. oxysporum

Considering that screening of a high number of transformants would be needed if *aldh* was disrupted using a vector lacking thymidine kinase (*hv-tk*), a negative selection vector (pPZP-*aldh-hyB*) harboring *hv-tk* was utilized. Supplementary Figure S1 shows the growth of the transformants on media containing F2dU and hygromycin. A total of 102 transformants were acquired on dual selection plates (Figure S1), with eight mutants exhibiting a colony diameter larger than 1.50 cm (Table 2).

Table 2. The resistance screening of *aldh* disrupted transformants using dual selectable markers. The mutants (T1–T8) were selected on PDA plate medium containing 100 μg/mL hygromycin, and then regenerated in the presence of 100 μg/mL hygromycin and 5-fluoro-2′-deoxyuridine (F2dU). +: growth.

Transformants	Hygromycin (100 μg/mL)	5-Fluoro-2′-Deoxyuridine (10 μM)	Diameter of Colony
T1	+	+	2.32
T2	+	+	2.10
T3	+	+	1.92
T4	+	+	1.85
T5	+	+	1.63
T6	+	+	1.55
T7	+	+	1.78
T8	+	+	1.93

For further identification of the transformants, the genomes of the mutants were extracted for PCR analysis using specific primer pairs P7/P8 and P1/P2 (Figure 3). The positions of primers P7/P8 and P1/P2 used to screen *F. oxysporum* transformants are indicated by solid arrows.

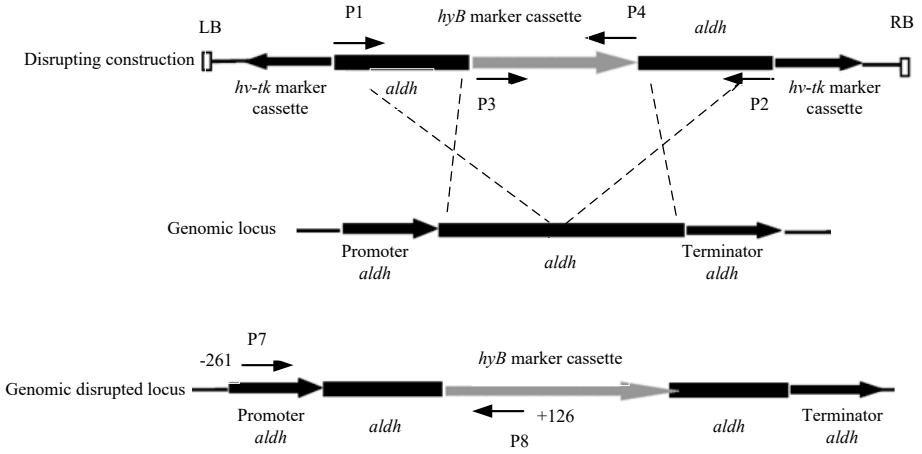

Figure 3. Schematic diagrams of strategy for disruption of *F. oxysporum aldh* in this study.

The numbers indicate the relative translation start codon (A of ATG as +1). P1–P8 indicate the PCR primers used to amplify the *aldh* and *hyB* cassette or to identify the disruption transformants. The *hv-tk* marker cassette included *Aspergillus nidulans* tryptophan C gene promoter (PtrpC), thymidine kinase gene from the herpes simplex virus (*hv-tk*), and *A. nidulans* tryptophan C terminator (TtrpC). The *hyg* marker cassette included PtrpC, *hyB*, and TtrpC. LB and RB indicate the left and right borders, respectively, of the T-DNA region in the binary vector pPZP-*aldh-hyB*.

Two transformants, T1 and T2 (lanes 1 and 2, respectively), and wild-type cs28 (lane 3) were firstly screened using PCR with specific primers P1 and P2 (lanes 1–3), and then

confirmed with primers P7 and P8 (lanes 4–6). The molecular weight markers are indicated in lanes M1 and M2. When the specific primers P1/P2 and P7/P8 were used, fragments of approximately 3.9 kb and 1.3 kb were acquired, respectively, suggesting that homologous recombination leading to gene disruption had occurred. Further, these fragments were sequenced by Sangon Biotech Co., Ltd., and the results were confirmed to be accurate (Figure 4).

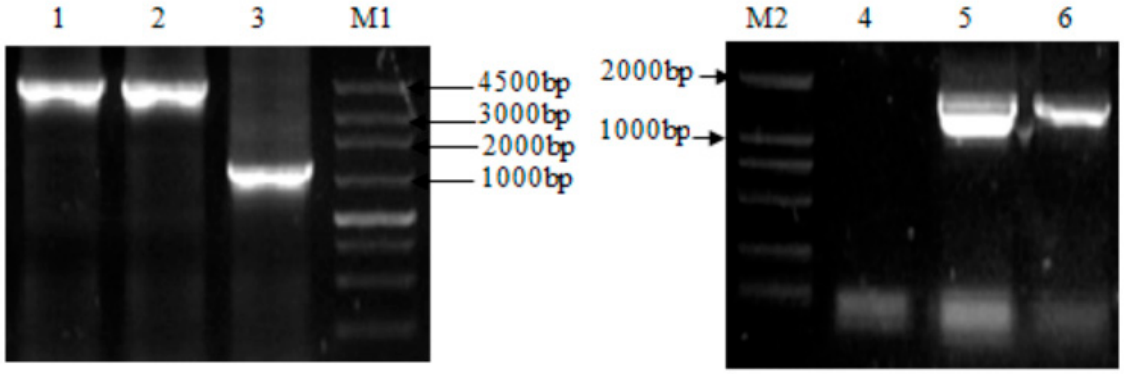

Figure 4. PCR amplification of wild-type strain and transformants. Two transformants, T1 (lanes 1 and 5) and T2 (lanes 2and 6), and wild-type strain (lanes 3 and 4) were firstly screened by PCR with specific primers P1and P2 (lanes 1–3) and then confirmed with primers P7 and P8 (lanes 4–6). M1: Marker 4500; M2: Marker 2000.

3.3. Sensitivity of the Mutants to Hygromycin and Their Mitotic Stability

A major prerequisite for the role of *hyB* as a selection marker in fungal transformation is the sensitivity of the host strain (*F. oxysporum* strain cs28) to hygromycin. To test this, either the spores or mycelia of the cs28 strain were inoculated on agar plates containing different concentrations of hygromycin. As shown in Table 2, the growth of *F. oxysporum* strain cs28 was inhibited at hygromycin concentrations higher than 50 μg/mL.

To identify whether knockout of *aldh* was stably inherited during vegetative growth, all mutants were grown for 1 week on PXA medium without hygromycin before being transferred back to PXA medium containing hygromycin. Growth without selection pressure did not affect the level of hygromycin resistance of any of the mutants, which indicated that the *aldh* knockout was mitotically stable. Furthermore, the mutants had a high resistance to hygromycin (100 μg/mL) (Table 3).

Table 3. Sensitivity of wild-type and putative mutants of *F. oxysporum* on hygromycin medium.

Strains	0	Hygromycin Concentration (μg/mL)			
		25	50	75	100
cs28	+	+	-	-	-
cs28pCAM-Ptal-Δald 13	+	+	+	+	+
cs28pCAM-Ptal-Δald 26	+	+	+	+	+

Samples were incubated for 7 days. cs28: wild-type strain; cs28pCAM-Ptal-Δ*aldh* 13 and cs28pCAM-Ptal-Δ*aldh* 26: mutants with plasmid (pPZP-*aldh*-hyB); +: growth; -: no growth.

3.4. Fermentation on Single-Sugar Medium

To determine the effect of disruption of *aldh* on *F. oxysporum*, 5 mL of the mutants were inoculated in glucose- and xylose-containing media in a 100 mL Erlenmeyer flask containing 50 mL of medium and cultivated statically at 30 °C under oxygen-limited conditions. The mutants were able to ferment glucose or xylose to produce ethanol as well as acetic acid as a by-product. There was a significant difference ($p < 0.01$) in ethanol production between the cs28pCAM-Pstal-Δ*aldh* and cs28 strains grown in glucose- and xylose-containing media. The ethanol yield of the wild-type strain in glucose- and xylose-containing media was 0.393

and 0.289 g/g, respectively. The ethanol yields in glucose- and xylose-containing media of cs28pCAM-Pstal-Δ*aldh* increased by 16.93% and 34.63% compared with the wild-type strain, respectively (Figure 5a and 5c). Furthermore, the ethanol production of cs28pCAM-Pstal-Δ*aldh* in glucose-containing media (9.15 g/L) and xylose-containing media (7.82 g/L) was 89.71% and 85% of the theoretical value, respectively.

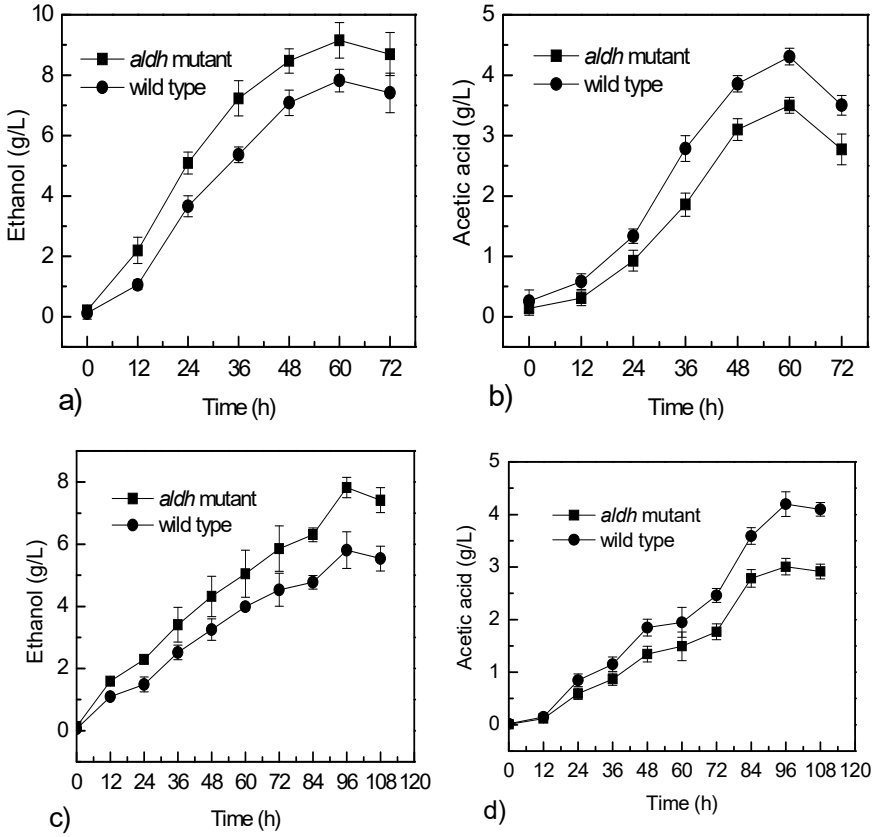

Figure 5. Time course of ethanol and acetic acid concentrations during metabolism of glucose and xylose with mutants. Glucose fermentation (**a**,**b**); Xylose fermentation (**c**,**d**). *square:* mutant strain cs28pCAM-Pstal-Δ*aldh*, *circle:* wild-type strain cs28.

A significant difference in acetic acid yield between the cs28pCAM-Pstal-Δ*aldh* and cs28 strains was observed in glucose-containing media ($p < 0.01$) and xylose-containing media ($p < 0.01$). The acetic acid yields of the wild-type strain in glucose- and xylose-containing media was 4.308 and 4.196 g/L, respectively. The acetic acid yields of cs28pCAM-Pstal-Δ*aldh* in glucose- and xylose-containing media decreased by 23.10% and 39.55% compared with that of the wild-type strain, respectively (Figure 5b,d). Furthermore, the acetic acid production of cs28pCAM-Pstal-Δ*aldh* in glucose-containing media (3.50 g/L) was higher than that in xylose-containing media (3.01 g/L).

A significant difference in substrate utilization between the cs28pCAM-Pstal-Δ*aldh* and cs28 strains was observed in glucose-containing media ($p < 0.05$) and xylose-containing media ($p < 0.01$). The concentrations of residual glucose and xylose in the media of cs28pCAM-Pstal-Δ*aldh* decreased by 30.30% and 29.45% compared with the wild-type strain, respectively (Figure 6a,b).

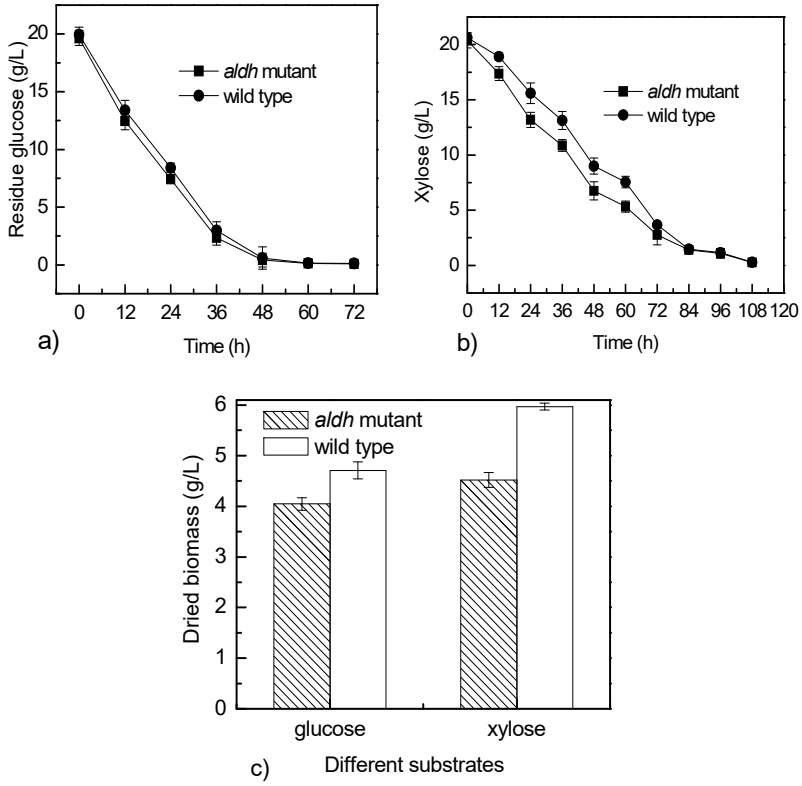

Figure 6. Xylose and glucose utilization and cell growth profile for *F. oxysporum* strain cs28 and mutant strain cs28pCAM-Pstal-Δ*aldh*. Cells were cultured in 50 mL of fermentation medium with 20 g/L of glucose (**a**) and 20 g/L of xylose (**b**), and dried biomass was weighed at 105 °C for 4 h (**c**). Symbols: ●: wild-type strain cs28; ■: *aldh* mutant strain cs28pCAM-Pstal-Δ*aldh*; □: wild-type strain cs28; ▨: *aldh* mutant strain cs28pCAM-Pstal-Δ*aldh*.

There was a significant difference ($p < 0.01$) in cell mass between the cs28pCAM-Pstal-Δ*aldh* and cs28 stains in glucose- and xylose-containing media (Figure 6c). The cell mass of the wild-type strain in glucose- and xylose-containing media was 4.71 and 5.97 g/L, respectively. The cell mass of the cs28pCAM-Pstal-Δ*aldh* strain decreased significantly compared with that of cs28 in both media ($p < 0.05$). One possible reason is that *aldh* deletion led to an increase in the NADH pool and disturbed the carbon flux to the biomass. Moreover, the cell mass of the mutants in xylose-containing media (4.52 g/L) was larger than that in glucose-containing media (4.04 g/L) (Figure 6c).

Gene replacement is commonly used to generate precise deletion mutants to investigate a possible function of the deleted gene. In addition to factors such as the length of homologous DNA in the gene replacement cassette, G/C content of these flanks, transcriptional status of the targeted gene, and chromatin structure determined by the location of the targeted gene on the chromosome, the transformation method used also affects the efficiency of the targeted integration. *Agrobacterium tumefaciens* mediated transformation (ATMT) has several advantages for gene manipulation in fungi, including high transformation efficiency and high homologous recombination frequency [26]. However, notably, gene disruption via homologous recombination was observed at a lower frequency [27]. Fungi with a low frequency of homologous recombination require the generation and screening of a large number of mutants for the identification of the desired mutant [28]. To circumvent this time-consuming process and facilitate the selection of homologous recombinants, a targeted gene replacement method based on ATMT followed by dual selection (positive and negative) of transformants was developed in this study. The *HSVtk* gene was originally used in animal cells to facilitate targeted gene replacement. It is a universal negative selection marker that has been utilized for testing many fungal species, such as *Leptosphaeria maculans* [21]. The *HSVtk* gene was chosen as a negative selectable marker

for rapid identification of the putative targeted integrations, irrespective of whether the locus conferred a selectable phenotype, and the *hyB* gene was selected as a positive marker. In this study, the putative homologous recombinants were easily selected by subjecting transformants to both positive (HYG) and negative (F2dU) selection agents to increase the screening efficiency (Figures 3 and 4). The screening results showed that the *HSVtk* could be used as a second selectable marker against ectopic transformants in *Fusarium* species.

Fusarium oxysporum, a well-known microorganism, can simultaneously saccharify straw to sugars and ferment sugars to ethanol. However, there are many bottlenecks that need to be addressed to increase the efficiency of its ethanol production from straw, such as the metabolic efficiency of xylose and glucose. The fermentative performance of various genetically modified *F. oxysporum* strains is presented in Table 4. Overexpression of the *tal* gene increased the ethanol yield of the transformants in xylose- and glucose-containing media; however, the acetic acid yield was also increased [11,12]. In *S. cerevisiae*, deletion of the *aldh* resulted in a decrease in acetic acid production [19]. These results were similar to those observed in this study (Figure 5b,d). The ethanol yield following glucose or xylose fermentation increased (Figure 5a,c). The mutants were mitotically stable and hence could be used in bioethanol production. However, there is a significant difference between bench-scale and industrial-scale batch fermentation. Determination and evaluation of the performance of an ethanol production process using the cs28pCAM-Pstal-Δ*aldh* strain will be essential in the future. Moreover, the fermentation ability of the mutants should be examined using sugar mixtures or lignocellulosic hydrolysates as substrates, and this could be a good strategy for cost reduction.

Table 4. Review of ethanol yield of different genetically modified *Fusarium oxysporum* strains and their fermentative performance in this study and from the literature.

Strains	Gene Up-Regulation/Down-Regulation	Substrates	Ethanol Yield (g/g)	Acetic Acid Yield (g/g)	Biomass (g/g)	References
F. oxysporum Fx13	endo-1,4-xylanase 2 /up-regulation	Corn cob	0.07	-	-	[29]
F. oxysporum Fx13	endo-1,4-xylanase 2 /up-regulation	Wheat bran	0.22	-	-	[29]
F. oxysporum cs28pCAM-Sctal4	transaldolase/ up-regulation	xylose	0.41	0.27	0.269	[12]
F. oxysporum cs28pCAM-Sctal4	transaldolase/ up-regulation	Rice straw	0.25	0.16	-	[12]
F. oxysporum FF11	phosphoglucomutase and transaldolase/ up-regulation	glucose	-	-	0.356	[13]
F. oxysporum FF11	phosphoglucomutase and transaldolase/ up-regulation	xylose		-	0.471	[13]
F. oxysporum pSilent-1-FoPTR2-3	peptide transporter/ down-regulation	Wheat straw	0.04		0.13	[6]
F. oxysporum pBARGPE1-FoPTR2-13	peptide transporter/ up-regulation	Wheat straw	0.09	-	0.18	[6]
F. oxysporum pBARGPE1-FoPTR2-13	peptide transporter/ up-regulation	glucose	0.4	-		[6]
F. oxysporum pBARGPE1-FoPTR2-13,	peptide transporter/ up-regulation	xylose	0.25	-		[6]
F. oxysporum pBARGPE1-Hxt-6	high affinity glucose transporter/ up-regulation	glucose	0.4	-		[10]
F. oxysporum pBARGPE1-Hxt-6	high affinity glucose transporter/ up-regulation	xylose	0.32	-		[10]
F. oxysporum cs28pCAM-Pstal-Δ*aldh*	aldehyde dehydrogenase/ down-regulation	glucose	0.45	0.175	0.202	The presentstudy
F. oxysporum cs28pCAM-Pstal-Δ*aldh*	aldehyde dehydrogenase/ down-regulation	xylose	0.39	0.15	0.226	The presentstudy

4. Conclusions

The *HSVtk* gene could be used as a second selectable marker against ectopic transformants in *Fusarium* species. The mutant strain cs28pCAM-Pstal-Δ*aldh* showed genetic stability. Moreover, it can ferment xylose and glucose to ethanol with a lower production of acetic acid (as a by-product) than the wild-type strain, indicating its potential as a microbial source for bioconversion of lignocellulose materials into bioenergy.

Supplementary Materials: The following supporting information can be downloaded at: https://www.mdpi.com/article/10.3390/en16010427/s1, Figure S1: The resistance screening of *aldh* disrupted transformants using dual selectable markers.

Author Contributions: Conceptualization, J.F. and Q.Y.; methodology, X.H.; formal analysis, G.Z.; investigation, G.Z. and C.L.; writing—original draft preparation, J.F. and C.L.; writing—review and editing, M.W.; supervision, Y.S. and Q.Y.; project administration, Q.Y. All authors have read and agreed to the published version of the manuscript.

Funding: This research was funded by the Science and Technology Program in Educational Department of Heilongjiang Province (No. 12511062), Postdoctoral Science Starting Funds Program of Heilongjiang Province (No. LBH-Q17021), Doctoral Starting Funds Program of Northeast Agricultural University (No. 2012RCB95) and Key Scientific and Technological Project of Heilongjiang Province of China (No. 2021ZXJ03B05).

Data Availability Statement: Not applicable.

Conflicts of Interest: The authors declare no conflict of interest.

References

1. Liu, C.; Sun, Y.; Yang, F.; Liu, J. Effect of solar irradiance on photo biochemical transformation process of direct absorption methane digester. *Energy Convers. Manag.* **2018**, *172*, 173–181. [CrossRef]
2. Singhvi, M.S.; Deshmukh, A.R.; Kim, B.S. Cellulase mimicking nanomaterial-assisted cellulose hydrolysis for enhanced bioethanol fermentation: An emerging sustainable approach. *Green Chem.* **2021**, *23*, 5064–5081. [CrossRef]
3. Rajak, R.C.; Saha, P.; Singhvi, M.; Kwak, D.; Kim, D.; Lee, H.; Deshmukh, A.R.; Bu, Y.; Kim, B.S. An eco-friendly biomass pretreatment strategy utilizing reusable enzyme mimicking nanoparticles for lignin depolymerization and biofuel production. *Green Chem.* **2021**, *23*, 5584–5599. [CrossRef]
4. Fu, Y.; Wu, P.; Xue, J.; Zhang, M.; Wei, X. Cosmosporasides F–H, three new sugar alcohol conjugated acyclic sesquiterpenes from a *Fusarium oxysporum* fungus. *Nat. Prod. Res.* **2022**, *36*, 3420–3428. [CrossRef]
5. Ibrahim, S.R.M.; Sirwi, A.; Eid, B.G.; Mohamed, S.G.A.; Mohamed, G.A. Bright Side of *Fusarium oxysporum*: Secondary Metabolites Bioactivities and Industrial Relevance in Biotechnology and Nanotechnology. *J. Fungi* **2021**, *7*, 943. [CrossRef]
6. Nugent, B.; Ali, S.S.; Mullins, E.; Doohan, F.M. A Major Facilitator Superfamily Peptide Transporter from *Fusarium oxysporum* Influences Bioethanol Production From Lignocellulosic Material. *Front. Microbiol.* **2019**, *10*, 295. [CrossRef]
7. Garzon, N.; Laure, H.J.; Rosa, J.C.; Cabral, H. *Fusarium oxysporum* cultured with complex nitrogen sources can degrade agricultural residues: Evidence from analysis of secreted enzymes and intracellular proteome. *Renew. Energy* **2018**, *133*, 941–950. [CrossRef]
8. Panagiotou, G.; Christakopoulos, P.; Villas-Boas, S.; Olsson, L. Fermentation performance and intracellular metabolite profiling of *Fusarium oxysporum* cultivated on a glucose–xylose mixture. *Enzym. Microb. Technol.* **2005**, *36*, 100–106. [CrossRef]
9. M'Barek, H.N.; Arif, S.; Taidi, B.; Hajjaj, H. Consolidated bioethanol production from olive mill waste: Wood-decay fungi from central Morocco as promising decomposition and fermentation biocatalysts. *Biotechnol. Rep.* **2020**, *28*, e00541. [CrossRef]
10. Ali, S.S.; Nugent, B.; Mullins, E.; Doohan, F.M. Insights from the Fungus *Fusarium oxysporum* Point to High Affinity Glucose Transporters as Targets for Enhancing Ethanol Production from Lignocellulose. *PLoS ONE* **2013**, *8*, e54701. [CrossRef]
11. Fan, J.X.; Yang, Q.; Liu, Z.H.; Huang, X.M.; Song, J.Z.; Chen, Z.X.; Sun, Y.; Liang, Q.; Wang, S. The characterization of transaldolase genetal from Pichia stipitis and its heterologous expression in *Fusarium oxysporum*. *Mol. Biol. Rep.* **2011**, *38*, 1831–1840. [CrossRef] [PubMed]
12. Fan, J.-X.; Yang, X.-X.; Song, J.-Z.; Huang, X.-M.; Cheng, Z.-X.; Yao, L.; Juba, O.S.; Liang, Q.; Yang, Q.; Odeph, M.; et al. Heterologous Expression of Transaldolase Gene Tal from *Saccharomyces cerevisiae* in *Fusarium oxysporum* for Enhanced Bioethanol Production. *Appl. Biochem. Biotechnol.* **2011**, *164*, 1023–1036. [CrossRef] [PubMed]
13. Anasontzis, G.E.; Kourtoglou, E.; Mamma, D.; Villas-Boâs, S.G.; Hatzinikolaou, D.G.; Christakopoulos, P. Constitutive homologous expression of phosphoglucomutase and transaldolase increases the metabolic flux of Fusarium oxysporum. *Microb. Cell Factories* **2014**, *13*, 43. [CrossRef]
14. Peng, H.; Wu, G.; Shao, W. The aldehyde/alcohol dehydrogenase (AdhE) in relation to the ethanol formation in *Thermoanaerobacter ethanolicus* JW200. *Anaerobe* **2008**, *14*, 125–127. [CrossRef] [PubMed]

15. Cao, Y.; Liao, L.; Xu, X.-W.; Oren, A.; Wu, M. Aldehyde dehydrogenase of the haloalkaliphilic archaeon *Natronomonas pharaonis* and its function in ethanol metabolism. *Extremophiles* **2008**, *12*, 849–854. [CrossRef] [PubMed]
16. Flipphi, M.; Mathieu, M.; Cirpus, I.; Panozzo, C.; Felenbok, B. Regulation of the Aldehyde Dehydrogenase Gene (aldA) and Its Role in the Control of the Coinducer Level Necessary for Induction of the Ethanol Utilization Pathway in *Aspergillus nidulans*. *J. Biol. Chem.* **2001**, *276*, 6950–6958. [CrossRef] [PubMed]
17. Remize, F.; Andrieu, E.; Dequin, S. Engineering of the Pyruvate Dehydrogenase Bypass in *Saccharomyces cerevisiae*: Role of the Cytosolic Mg^{2+} and Mitochondrial K^{+} Acetaldehyde Dehydrogenases Ald6p and Ald4p in Acetate Formation during Alcoholic Fermentation. *Appl. Environ. Microbiol.* **2000**, *66*, 3151–3159. [CrossRef] [PubMed]
18. Wang, X.; Mann, C.J.; Bai, Y.; Ni, L.; Weiner, H. Molecular cloning, characterization, and potential roles of cytosolic and mi-tochondrial aldehyde dehydrogenases in ethanol metabolism in *Saccharomyces cerevisiae*. *J. Bacteril.* **1998**, *180*, 822–830. [CrossRef]
19. Lu, X.H.; Wang, D.L.; Fu, L.; Zhao, C.S. Gene deletion to decrease acetic acid of *Saccharomyces cerevisiaes*. *Liquor. Mak. Sci. Technol.* **2007**, *3*, 41–44.
20. Staben, C.; Jensen, B.; Singer, M.; Pollock, J.; Schechtman, M.; Kinsey, J.; Selker, E. Use of a bacterial hygromycin B resistance gene as a dominant selectable marker in *Neurospora crassa* transformation. *Fungal Genet. Newsl.* **1989**, *36*, 79–81. [CrossRef]
21. Gardiner, D.M.; Howlett, B.J. Negative selection using thymidine kinase increases the efficiency of recovery of transformants with targeted genes in the filamentous fungus *Leptosphaeria maculans*. *Curr. Genet.* **2004**, *45*, 249–255. [CrossRef] [PubMed]
22. Jyothishwaran, G.; Kotresha, D.; Selvaraj, T.; Srideshikan, S.; Rajvanshi, P.; Jayabaskaran, C. A modified freeze–thaw method for efficient transformation of *Agrobacterium tumefaciens*. *Curr. Sci.* **2007**, *93*, 770–772. Available online: https://www.currentscience.ac.in/Volumes/93/06/0770.pdf (accessed on 26 December 2022).
23. Covert, S.F.; Kapoora, P.; Holeea, M.; Brileya, A.; Nairn, C.J. *Agrobacterium tumefaciens*-mediated transformation of *Fusarium circinatum*. *Mycol. Res.* **2001**, *105*, 259–264. [CrossRef]
24. Karakousis, A.; Tan, L.; Ellis, D.; Alexiou, H.; Wormald, P. An assessment of the efficiency of fungal DNA extraction methods for maximizing the detection of medically important fungi using PCR. *J. Microbiol. Methods* **2006**, *65*, 38–48. [CrossRef]
25. Zhao, L.; Zhang, X.; Tan, T. Influence of various glucose/xylose mixtures on ethanol production by *Pachysolen tannophilus*. *Biomass Bioenergy* **2008**, *32*, 1156–1161. [CrossRef]
26. Michielse, C.; Arentshorst, M.; Ram, A.; Hondel, C.V.D. Agrobacterium-mediated transformation leads to improved gene replacement efficiency in *Aspergillus awamori*. *Fungal Genet. Biol.* **2005**, *42*, 9–19. [CrossRef]
27. Ma, J.-C.; Zhou, Q.; Zhou, Y.-H.; Liao, X.-G.; Zhang, Y.-J.; Jin, D.; Pei, Y. The size and ratio of homologous sequence to non-homologous sequence in gene disruption cassette influences the gene targeting efficiency in *Beauveria bassiana*. *Appl. Microbiol. Biotechnol.* **2009**, *82*, 891–898. [CrossRef]
28. Mullins, E.D.; Kang, S. Transformation: A tool for studying fungal pathogens of plants. *Cell. Mol. Life Sci. CMLS* **2001**, *58*, 2043–2052. [CrossRef]
29. Anasontzis, G.E.; Zerva, A.; Stathopoulou, P.M.; Haralampidis, K.; Diallinas, G.; Karagouni, A.D.; Hatzinikolaou, D.G. Homologous overexpression of xylanase in Fusarium oxysporum increases ethanol productivity during consolidated bioprocessing (CBP) of lignocellulosics. *J. Biotechnol.* **2011**, *152*, 16–23. [CrossRef]